

Accepted Manuscript

Optimization of Dipeptidic Inhibitors of Cathepsin L for Improved *Toxoplasma gondii* Selectivity and CNS Permeability

Jeffery D. Zwicker, Nicolas A. Diaz, Alfredo J. Guerra, Paul D. Kirchhoff, Bo Wen, Duxin Sun, Vern B. Carruthers, Scott D. Larsen

PII: S0960-894X(18)30199-9
DOI: <https://doi.org/10.1016/j.bmcl.2018.03.020>
Reference: BMCL 25674

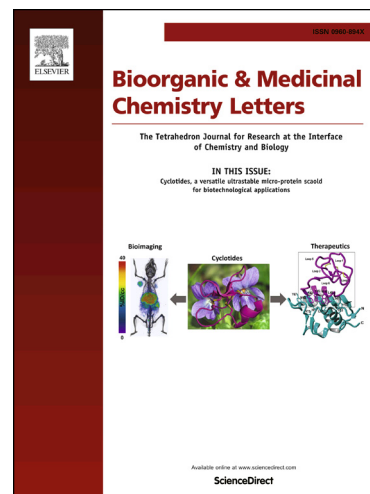
To appear in: *Bioorganic & Medicinal Chemistry Letters*

Received Date: 26 January 2018

Accepted Date: 7 March 2018

Please cite this article as: Zwicker, J.D., Diaz, N.A., Guerra, A.J., Kirchhoff, P.D., Wen, B., Sun, D., Carruthers, V.B., Larsen, S.D., Optimization of Dipeptidic Inhibitors of Cathepsin L for Improved *Toxoplasma gondii* Selectivity and CNS Permeability, *Bioorganic & Medicinal Chemistry Letters* (2018), doi: <https://doi.org/10.1016/j.bmcl.2018.03.020>

This is a PDF file of an unedited manuscript that has been accepted for publication. As a service to our customers we are providing this early version of the manuscript. The manuscript will undergo copyediting, typesetting, and review of the resulting proof before it is published in its final form. Please note that during the production process errors may be discovered which could affect the content, and all legal disclaimers that apply to the journal pertain.



Optimization of Dipeptidic Inhibitors of Cathepsin L for Improved *Toxoplasma gondii* Selectivity and CNS Permeability

Jeffery D. Zwicker^{a,b}, Nicolas A. Diaz^{a,b}, Alfredo J. Guerra^c, Paul D. Kirchhoff^b, Bo Wen^d, Duxin Sun^d, Vern B. Carruthers^c, and Scott D. Larsen^{a,b}

^aVahlteich Medicinal Chemistry Core, College of Pharmacy, University of Michigan, Ann Arbor, Michigan 48109, United States

^bDepartment of Medicinal Chemistry, University of Michigan, Ann Arbor, Michigan 48109, United States

^cDepartment of Immunology and Microbiology, University of Michigan, Ann Arbor, Michigan 48109, United States

^dPharmacokinetics Core, Department of Pharmaceutical Sciences, University of Michigan, Ann Arbor, Michigan 48109, United States

*Corresponding author. Tel: 734-615-0454

E-mail addresses: sdlarsen@med.umich.edu

KEYWORDS: *Toxoplasma gondii*, toxoplasmosis, cathepsin L, protease, infectious disease, antiprotazoal agents, blood-brain-barrier, central nervous system

Abstract

The neurotropic protozoan *Toxoplasma gondii* is the 2nd leading cause of death due to foodborne illness in the US, and has been designated as one of five neglected parasitic infections by the Center for Disease Control and Prevention. Currently, no treatment options exist for the chronic dormant-phase *Toxoplasma* infection in the central nervous system (CNS). *T. gondii* cathepsin L (TgCPL) has recently been implicated as a novel viable target for the treatment of chronic toxoplasmosis. In this study, we report the first body of SAR work aimed at developing potent inhibitors of TgCPL with selectivity vs the human cathepsin L. Starting from a known inhibitor of human cathepsin L, and guided by structure-based design, we were able to modulate the selectivity for *Toxoplasma* vs human CPL by nearly 50-fold while modifying physiochemical properties to be more favorable for metabolic stability and CNS penetration. The overall potency of our inhibitors towards TgCPL was improved from 2 μ M to as low as 110 nM and we successfully demonstrated that an optimized analog **18b** is capable of crossing the BBB (0.5 brain/plasma). This work is an important first step toward development of a CNS-penetrant probe to validate TgCPL as a feasible target for the treatment of chronic toxoplasmosis.

With an estimated two billion people chronically infected, *Toxoplasma gondii* is one of the most pervasive infectious agents in the world.^{1, 2} This neurotropic protozoan is the 2nd leading cause of death due to foodborne illness in the US, and has been designated as one of five neglected parasitic infections targeted by the Center for Disease Control and Prevention for public health action.³⁻⁵ In its mammalian hosts, *T. gondii* exists in two principal forms, the tachyzoite and bradyzoite. The initial disease state is caused by the rapidly replicating tachyzoite form. This stage typically lasts for a several days to weeks during which the parasite disseminates to peripheral sites including the central nervous system (CNS). *T. gondii* then transitions into a chronic bradyzoite cyst form within the CNS and muscle tissue to establish life-long infection.^{6, 7} This chronic stage infection was once considered to be benign, but recent studies have identified associations with variety of host behavioral changes and mental illnesses including schizophrenia, bipolar disorder, and obsessive compulsive disorder.⁸⁻¹² In the case of immunocompromised hosts (e.g. chemotherapy patients and HIV-positive individuals), the parasite cysts can reactivate into the active tachyzoite form, leading to more serious complications such as, encephalitis, blindness, and death.^{1, 13, 14} Currently, there is no efficacious *T. gondii* therapeutic capable of treating the chronic-phase infection. Given the limitations and current inadequacies of antiparasitic therapies, there is a serious need for the development of novel and alternative strategies for the treatment of chronic *T. gondii* infection.

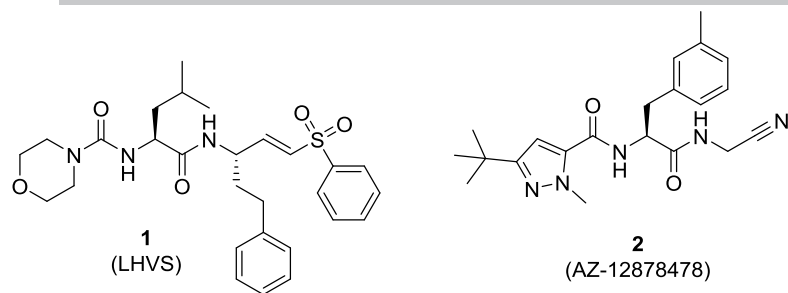


Figure 1. Literature Lead Cathepsin L Inhibitors.

Inhibition of vital cysteine proteases is an increasingly attractive approach for the treatment of various disease states caused by protozoans such as *Trypanosoma cruzi*, *Plasmodium falciparum*, and others.¹⁵⁻¹⁷ Recently, we demonstrated that *T. gondii* cathepsin protease L (TgCPL) is critical to parasite survival during the chronic phase of infection.^{18, 19} Inhibition of TgCPL in tissue culture by the irreversible inhibitor morpholinurea-leucine-homophenylalaninevinyl phenyl sulfone **1** (LHVS) (**Figure 1**) kills *T. gondii* cysts, further implicating TgCPL as a viable target for treatment of the chronic stage infection. Unfortunately, LHVS is unable to cross the blood brain barrier precluding its use as a proof-of-concept probe in infected mice.²⁰ Additionally, LHVS is a nonselective and irreversible inhibitor, increasing the possibility of off-target effects and poor selectivity across cathepsin isoforms.

An enormous amount of drug discovery and development has been done in regard to both human and parasitic cathepsins isoforms, and extensive mechanistic and structural information is available.²¹⁻²⁸ Given the close homology between the human and parasitic isoforms of cathepsin L, we considered the vast libraries of inhibitors already developed against human isoforms to be a promising source of lead anti-parasitic compounds.²⁹ To identify a better potential lead compound than LHVS, we conducted a broad literature search of structurally diverse CPL inhibitors emphasizing physicochemical properties predictive of CNS permeability, selectivity over other human cathepsins, and potency ($IC_{50} < 1 \mu M$).

Table 1. Comparison of calculated properties of lead inhibitors vs CNS and non-CNS drugs

Compound	MW	SlogP	tPSA	HBA	HBD	RotB
CNS drug	288 ± 88	2.8 ± 1.4	46 ± 26	2.6 ± 1.3	1.0 ± 0.9	4.0 ± 2.6
non-CNS drug	383 ± 210	2.1 ± 2.9	98 ± 84	4.8 ± 4.1	2.8 ± 3.3	6.2 ± 5.5
1	527.69	3.6	104.8	5	2	14
2	381.48	2.4	99.8	4	2	10

Calculated using The Molecular Operating Environment (MOE), version 2008.10, Chemical Computing Group Inc., Montreal, Quebec, Canada.³⁰ Mean values and standard deviations derived from 198 approved CNS drugs and 1015 approved non-CNS drugs (DrugBank).

We ultimately selected our initial lead compound **2** (**Figure 1**) based on its calculated properties: molecular weight (MW), topological polar surface area (tPSA), numbers of hydrogen bond acceptors and donors (HBA, HBD), and rotatable bonds (RotB), which are collectively closer to marketed CNS drugs vs non-CNS drugs than are those of LHVS and most other literature leads we considered (**Table 1**)³¹. In addition, we considered the ease with which we could expect to improve predicted BBB access by further lowering the tPSA.

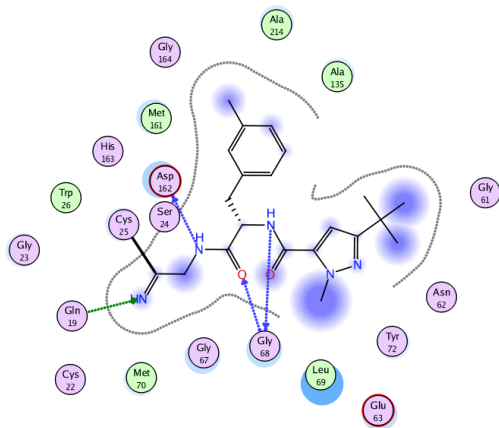


Figure 2. LIGPLOT (right) diagram generated in MOE, shows key interactions between **2** and HsCPL. Hydrogen bonds: blue arrows, lipophilic interactions: blue spheres. Derived from PDB: 3HHA

As the first ever SAR campaign targeting TgCPL, we elected to use a dipeptide nitrile scaffold as our lead, based on the extensive amount of dipeptide-type cathepsin inhibitors previously developed for related human isoforms.³²⁻³⁴ We believed the use of dipeptide probes would enable rapid elucidation of the pharmacophore necessary for the selective inhibition of TgCPL due to their synthetic accessibility and ease of diversity introduction. Another key rationale for selecting **2** as our lead was the aminoacetonitrile “warhead”. The majority of small molecule protease inhibitors incorporate a functional group that can react with the active site cysteine or serine in a reversibly covalent manner that imparts high affinity with relatively low off-target reactivity.^{32, 35, 36} The aminoacetonitrile group has been extensively studied and is present in a number of FDA-approved drugs and advanced clinical candidates, including vildagliptin, saxagliptin, and odanacatib.³⁷ Furthermore, its low molecular weight and relatively low tPSA were considered advantageous for achieving CNS permeability.

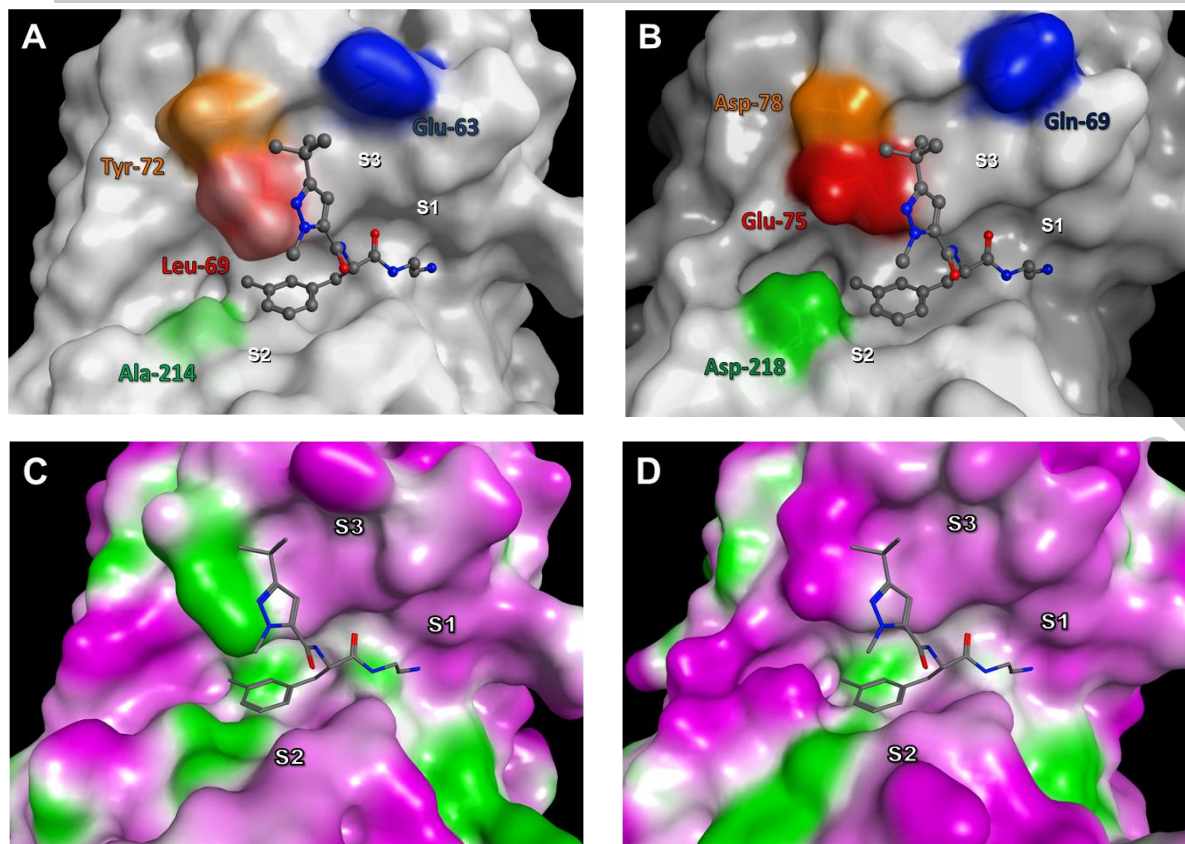
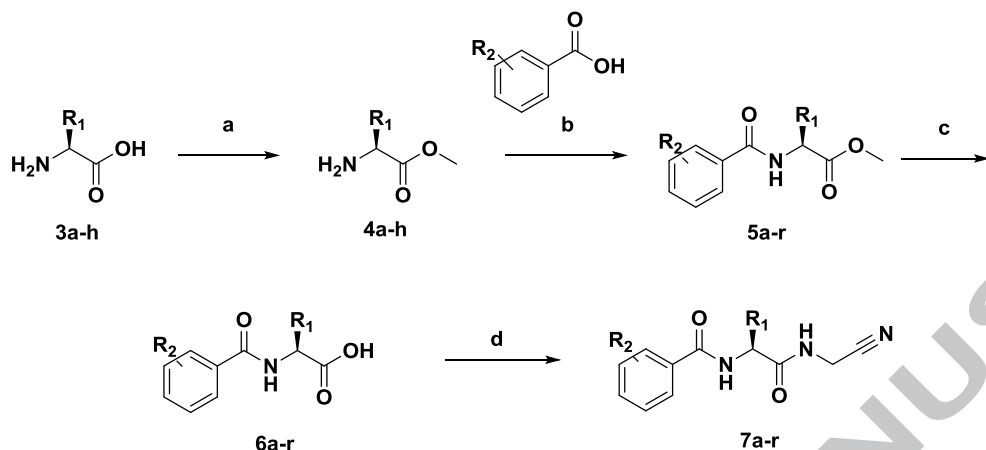


Figure 3. Comparison of **2** bound to HsCPL (A, C) and a superposition of **2** modeled into the active site of TgCPL (B, D) depicting key non-conserved residues. A) HsCPL with key residues colored. B) TgCPL with key residues colored C) Lipophilicity mapping of HsCPL (green: lipophilic; magenta: polar); D) Lipophilicity mapping of TgCPL. (Derived from PDB codes: 3HHA and 3F75)

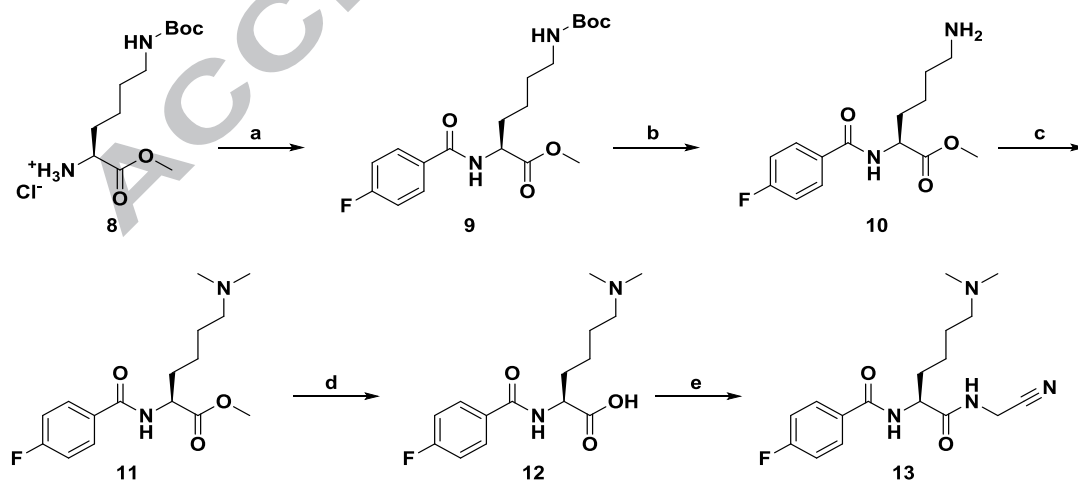
Finally, we selected **2** as a lead because of the availability of an X-ray co-crystal structure of it bound to human cathepsin L (HsCPL, (PDB: 3HHA)).³¹ Opportunely, a crystal structure of TgCPL was also available from our previous work, which we expected would greatly facilitate the design of TgCPL-selective inhibitors.^{31, 38-41} The crystal structure of **2** bound to HsCPL shows that the active site Cys25 is covalently added to the nitrile, consistent with other reversibly-covalent nitrile based inhibitors of cysteine proteases, and that the ligand makes hydrogen-bonding interactions with Asp162, Gly68, and Gln19 (**Figure 2**).^{32, 35} Importantly, the bound inhibitor **2** can be overlaid on our crystal structure of TgCPL to identify proximal structural differences between the cathepsins that can be exploited to achieve selective inhibition of the *T. gondii* enzyme (**Figure 3**).¹⁸ In particular this overlay reveals a smaller S2 pocket for the *Toxoplasma* cathepsin, as well as four non-conserved residues (colored in **Figures 3A,B**). Further comparison of the protein sequence alignment of TgCPL and the human cathepsin isoforms A-X, revealed that these key residues are either unique to TgCPL, or generally non-conserved across human isoforms. The S2 pocket across the human cathepsins tends to be more uniformly lipophilic (colored green in **Figures 3C,D**) than TgCPL, and the inclusion of a basic residue in the P2 position, which we predicted might interact strongly with non-conserved Asp-218 in TgCPL, is generally not tolerated. With the exception of human cathepsin B, which bears a Glu245 in this respective position, the overall topology in the S2 subsite is thus substantially different than that of TgCPL.⁴² This provided excellent supporting evidence that optimization in the P2 position would be paramount in an effort to gain selectivity over the bulk of the human isoforms.

Our primary objectives in this preliminary work were: 1) to develop analogs with better predicted CNS permeability without losing potency; and 2) to determine if we can begin to shift the selectivity of **2** away from HsCPL and towards TgCPL. Herein we report the development of a series of dipeptide nitrile probes that help to define pharmacophoric features key to improving both potency and selectivity for TgCPL, including one analog with CNS permeability in vivo.



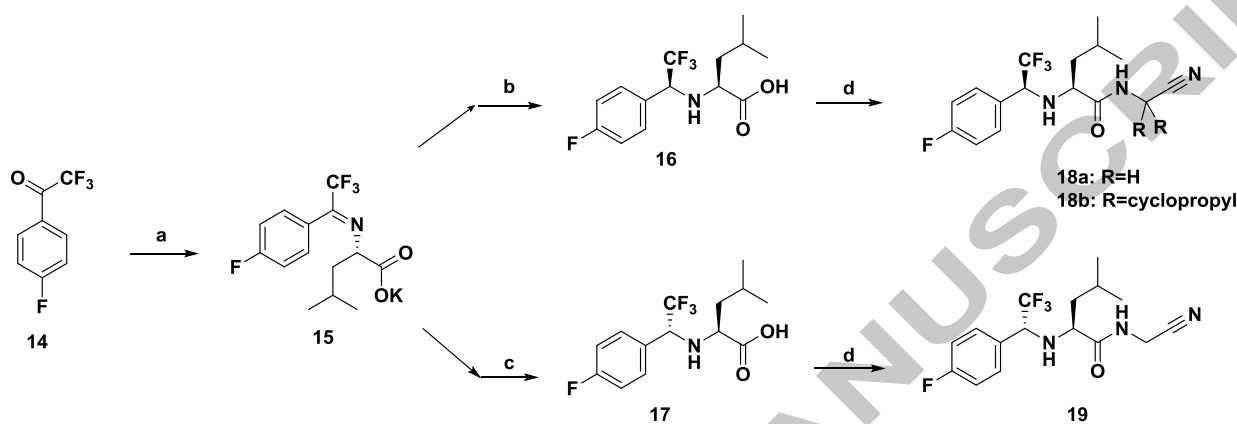
Scheme 1. General synthesis of dipeptide nitriles. Reagents and conditions: a) H_2SO_4 , MeOH, reflux; b) HATU, DIPEA, DMF; c) 1N $\text{LiOH}_{(\text{aq})}$, THF, MeOH; d) 2-aminoacetonitrile bisulfate, HATU, DIPEA, DCM, 0°C -rt

Synthesis of analogs **7a-r** (**Scheme 1**) was performed analogous to the literature precedent for the peptide-nitrile cathepsin inhibitors.^{31, 32, 34, 41} We began with the esterification of various commercially available L-amino acids **3a-h** to afford their respective methyl esters **4a-h**. Subsequent amide coupling to the appropriate aryl acids gave **5a-r**. The methyl ester was then saponified under mild conditions with LiOH in a THF:MeOH system to afford the desired free acid **6a-r**. Initial coupling with 2-aminoacetonitrile gave several unwanted side reactions and generally low yields when using DMF or THF as the solvent, regardless of the temperature or coupling reagent used. Upon changing to dichloromethane we found that, while solubility was not always ideal, the desired products **7a-r** were formed cleanly and in moderate yields.



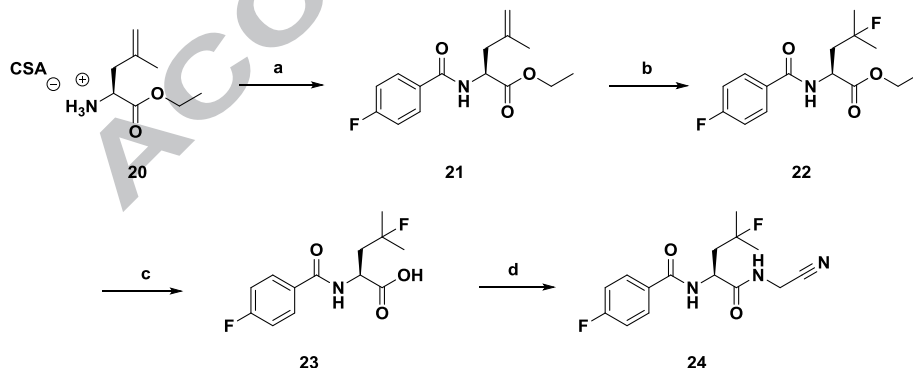
Scheme 2. Synthesis of dimethyl-lysine analog. Reagents and conditions: a) 4-Fluorobenzoic acid, HATU, DIPEA, DMF, 98%; b) 4N HCl/dioxane, 99%; c) formaldehyde, sodium triacetoxyborohydride, MeOH, 32%; d) 1N LiOH_(aq), THF, MeOH, 100%; e) 2-aminoacetonitrile bisulfate, HATU, DIPEA, DCM, 0°C-rt, 11%.

Synthesis of **13** was achieved as shown in **Scheme 2**. N ϵ -Boc-L-lysine methyl ester hydrochloride **8** was coupled to 4-fluorobenzoic acid to provide intermediate **9**. Boc removal from **9** afforded the HCl salt of **10** which was immediately followed by dimethylation of the sidechain to provide compound **11**. Saponification of **11** with lithium hydroxide provided **12**, and subsequent amide coupling using HATU gave the desired product **13**.



Scheme 3. Reagents and conditions: a) Leucine hydrochloride, K₂CO₃, MeOH, 50°C, 18h; b) Zn(BH₄)₂, ACN/DME, -40°C, 5h, 87%; c) NaBH₄, THF, 93%; d) 2-aminoacetonitrile bisulfate, or 1-aminocyclopropane-1-carbonitrile HCl, HATU, DIPEA, DCM, 0°C-rt, 45-89%

Trifluoroethyl amine analogs (**18a-b**, **19**) were generally synthesized as shown in **Scheme 3** following previously established methods in the development of odanacatib.^{43, 44} Synthesis began with the condensation of the trifluoroacetophenone **14** and L-Leucine-methylester under basic conditions to afford the imine intermediate **15**. The *R,S* diastereomer **17**, was obtained via dropwise addition of NaBH₄ dissolved in THF at -40°C in a 10:1 dr. Alternatively the (*S,S*) diastereomer could be obtained through a chelation controlled reduction of the imine with zinc borohydride in acetonitrile/dimethoxyethane at -40°C, providing **16** in an 11:1 dr. The (*S,S*) and (*R,S*) compounds **18a**, **18b**, and **19** were obtained in 45-94% yield through the previously described amide coupling conditions (**Scheme 1**).



Scheme 4. Reagents and conditions: a) 4-fluorobenzoic acid, HATU, DIPEA, DMF, 34%; b) Selectfluor, Fe₂(SO₄)₃, NaBH₄, acetonitrile:water, 0°C-rt, 27%; c) 1N LiOH_(aq), THF:EtOH, 0°C-rt, 100%; d) 2-aminoacetonitrile bisulfate, HATU, DIPEA, DCM, 0°C-rt, 18%

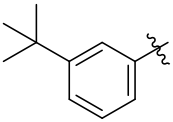
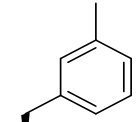
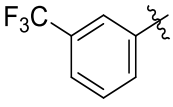
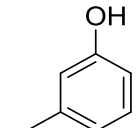
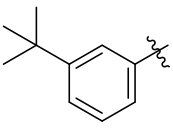
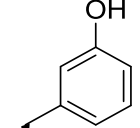
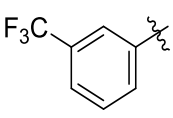
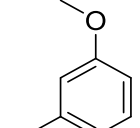
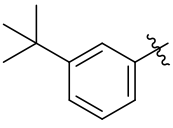
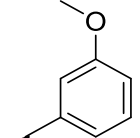
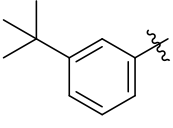
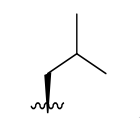
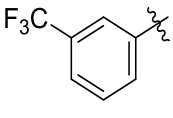
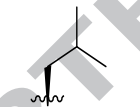
Fluoroleucine analog **24** was prepared as shown in **Scheme 4** through a sequence derived from previously reported methods for analogous compounds.⁴⁴⁻⁴⁷ Dehydroleucine **20**, as the CSA salt, was coupled to 4-fluorobenzoic acid to provide intermediate amide **21**. Initially, we tried to achieve fluorination of **21** using a variety of the previously reported conditions, predominantly using reagents that are a source of nucleophilic fluorine such as HF:Urea or HF:Pyridine. However, these conditions generally suffered from poor yields and unwanted side reactions such as cyclization or elimination. We then opted to try an electrophilic source of fluorine as an alternative approach, derived from that reported by Fanelli et. al.⁴⁸ Activation of the olefin with Fe(III), followed by the sequential addition of Selectfluor and NaBH₄ provided the desired product **22** in moderate which, was then saponified to **23** and directly coupled to 2-aminoacetonitrile, affording the desired compound **24**.

All new compounds were evaluated in vitro for inhibition of both TgCPL and HsCPL activity by monitoring the rates of hydrolysis of Z-Leu-Arg-7-amino-4-methylcoumarin (Z-L-R-AMC). Results are summarized in Tables 2-5. We first re-synthesized literature lead **2** to benchmark its relative potency against TgCPL versus HsCPL. In vitro testing revealed low micromolar potency against TgCPL, and 46-fold more potent inhibition against HsCPL (**Table 2**).

Initially we replaced the pyrazole heterocycle in the P3 position of **2** with phenyl in order to remove two nitrogen atoms (**7b**) and rapidly lower the tPSA of **2**, thereby increasing the potential for CNS permeability. This exchange resulted in a 2-3-fold drop in potency against HsCPL while enhancing activity against TgCPL, improving the TgCPL-selectivity about 4-fold. The t-butyl group of **7b** was then replaced by trifluoromethyl to stabilize the now electron-rich P3 aromatic ring to potential oxidation by CYP450 enzymes, giving **7a**. This analog lost potency against TgCPL, but maintained effectiveness versus HsCPL. Since both of these analogs had reduced selectivity for HsCPL compared to lead **2** we retained both of the P3 groups during our initial survey of P2.

Table 2. Cathepsin L inhibitory activity of initial P2 and P3 analogs.

Name	Ar	R	TgCPL ^a IC ₅₀ (μM)	HsCPL ^b IC ₅₀ (μM)	Selectivity for HsCPL ^c
1	N/A	N/A	0.002	0.003	0.7
2			2.0	0.044	46.4
7a			2.4	0.11	22.5

7b			1.4	0.13	11.3
7c			1.4	0.042	33.5
7d			1.2	0.092	13.3
7e			6.1	0.086	71
7f			4.6	0.24	18.8
7g			0.12	0.077	1.9
7h			0.12	0.32	0.4

^{a,b}IC₅₀ for *Toxoplasma gondii* Cathepsin L (TgCPL) or human Cathepsin L (HsCPL). Values are mean of at least 3 independent experiments. ^cSelectivity ratio for human Cathepsin L as defined by TgCPL IC₅₀/HsCPL IC₅₀.

The vast majority of selectivity between human cathepsin isoforms comes from the P2-S2 interaction.⁴⁹ The S3 and S1 subsites also play significant roles in inhibitor selectivity, while the S' subsites (toward the C-terminus of the scissile bond) are highly conserved between isoforms and generally difficult to exploit.²² Inspection of the cathepsin crystal structures revealed several active site residues unique to the *T. gondii* isoform vs the human isoform that could potentially be exploited to gain selectivity and potency. As noted above, the TgCPL S2 site contains a unique aspartate residue (Asp218), as opposed to the human isoform, which bears a hydrophobic alanine in this position (colored green in **Figures 3A, B**). Overlaying TgCPL with the co-crystal structure of our lead compound bound to HsCPL indicates that the 3-methylphenylalanine (3-Me-Phe) core of **2** sits approximately 3-4 Å from this key aspartate (Figure 3B). Due to the proximity of the core to Asp218 we hypothesized we might be able to build in a potential H-bond to improve potency and selectivity.

The P2 3-methylphenylalanine residue of analogs **7a** and **7b** was thus replaced with 3-hydroxyphenylalanine or 3-methoxyphenylalanine (**7c-7f**) in an attempt to pick up a selective hydrogen bonding interaction with the non-conserved Asp218 of TgCPL. We had hoped this would provide some initial gain in selectivity toward the parasite cathepsin, but the results were inconsequential changes in potency. This might be due to the rigidity of the Asp218 backbone orienting the residue away from the S2 pocket and preventing a beneficial interaction.

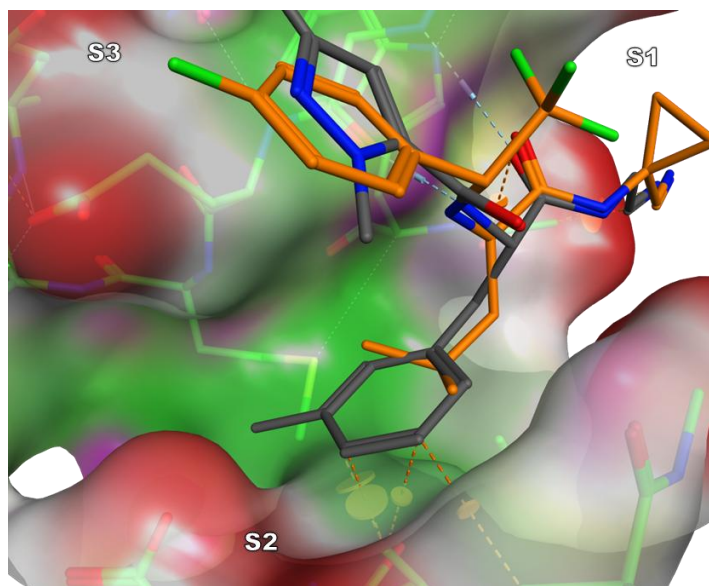
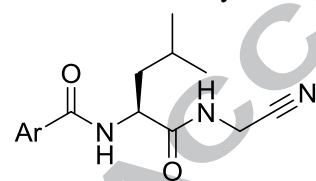


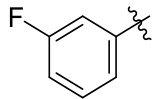
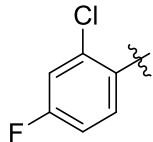
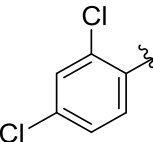
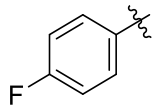
Figure 4. Overlay of **2** (gray) and **18b** (orange) into the crystal structure of TgCPL (PDB code: 3F75) depicting clashes with **2** in the S2 pocket. Hydrogen bonds and clashes are represented as blue and orange dashed lines, respectively. Pocket surface coloration represents polar (purple), lipophilic (green), and solvent exposed (red) areas.

Molecular modeling also identified several predicted clashes with HsCPL when the larger phenylalanine side chains are in the P2 position (**2** in **Figure 4**). We were pleased to discover that replacement of the entire aromatic P2 residue with a less bulky leucine (**7g,7h**) significantly reduced selectivity for HsCPL, consistent with the smaller S2 subsite in the TgCPL as compared to the human isoform (Table 2). With this single change, we reduced the selectivity of **2** for HsCPL from 10-20 fold to <2 fold. This is an excellent validation that the differences in the S2 pockets can be exploited for improving TgCPL selectivity.

Table 3. Inhibitory activity of additional aryl P3 substitution analogs.



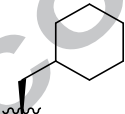
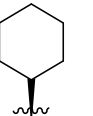
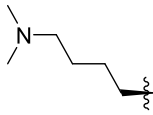
Name	Ar	TgCPL ^a IC ₅₀ (μ M)	HsCPL ^b IC ₅₀ (μ M)	Selectivity for HsCPL ^c
7i		0.35	0.11	3.3
7j		0.18	0.015	11.7

7k		0.36	0.048	7.6
7l		0.54	0.28	1.9
7m		0.53	0.14	3.8
7n		0.25	0.28	0.9

^{a,b,c}See Table 2 for heading definitions.

We then returned to optimization of the P3 position in an effort to reduce the molecular weight of **7h** while retaining a halogenated pendant for metabolic stability (Table 3). Removal of the trifluoromethyl from the P3 pendant to afford the simple phenyl (**7i**) unfortunately reversed the selectivity back to HsCPL over TgCPL. A similar trend was observed with analogs **7j**, **7l**, and **7m**, which bear a 3-methyl, 2-chloro-4-fluoro, or 2,4-dichloro substitution pattern, respectively, on the P3 pendant. Replacement of the 3-trifluoromethyl of **7h** with a fluorine (**7k**) also resulted in a large drop in potency for TgCPL and an increase for the human isoform. The 4-fluoro analog **7n**, however, was equipotent at TgCPL and HsCPL, and lowered the MW below 300, making this a more promising candidate for CNS permeability as compared to the somewhat more potent and TgCPL-selective 4-trifluoromethyl analog **7h**.

Table 4. Inhibitory activity of additional aliphatic P2 analogs

Name	R	TgCPL ^a IC ₅₀ (μ M)	HsCPL ^b IC ₅₀ (μ M)	Selectivity for HsCPL ^c
7o		0.42	0.19	2.3
7p		6.6	1.2	5.7
13		14	816	0.02

24		4.0	2.5	1.6
25		2.0	1.2	1.6
7q		1.2	3.5	0.3
7r		9.8	4.1	2.4

^{a,b,c}See Table 2 for heading definitions.

We then explored a dimethyl lysine at P2 as a basic group to establish a salt bridge with the non-conserved Asp218 of TgCPL (**13** in **Table 4**). While this was predicted by modeling to be the optimal length to interact with the S2 aspartic acid, it nevertheless resulted in a major loss in potency against both isoforms. However, it should be noted that the loss in potency was significantly greater against the human isoform, demonstrating that despite the S2 pocket of these two enzymes being very similar, subtle differences at the P2 residue can offer drastic changes to the selectivity profile. Further exploration of basic residues at P2 is therefore warranted in future SAR studies.

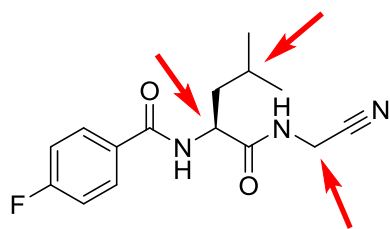
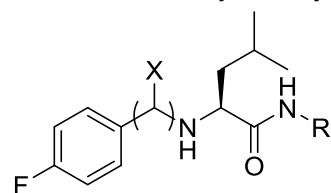


Figure 5. SMARTCyp prediction of the top three sites of metabolism.

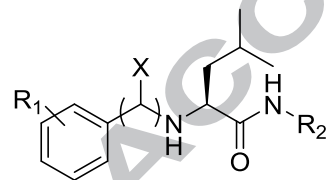
Cyclohexyl P2 analogs have been reported as inhibitors of human protease inhibitors that offered some improvement in either binding or metabolic stability.⁵⁰ To further probe aliphatic SAR at the TgCPL P2 position, both were made (**7o** and **7p**, **Table 4**); however, neither offered any improvement. Rather, a decrease in potency and TgCPL selectivity was observed for both, more drastically in the case of **7p**, which is a closer mimic of valine than leucine. Substitutions much larger than leucine were thus apparently not well tolerated in TgCPL, consistent with the poor activity we had observed earlier with our phenylalanine analogs, so we attempted to install isosteres that were closer in size to leucine. While the use of fluoroleucine to improve metabolic issues has been successfully demonstrated in the development of odanacatib⁵¹, we were surprised to see a drastic drop in potency against both TgCPL (IC_{50} = 4.05 μ M) and HsCPL (IC_{50} = 2.51 μ M) with compound **24**. Similarly, exchange of the P2 leucine with either a neopentylglycine, or dehydroleucine (**7q**, **25**) resulted in a significant loss of potency (IC_{50} = 1.19 μ M and 2.00 μ M respectively). Surprisingly, even the cyclopropyl analog **7r** showed a large drop in potency as compared to **7n**. While these structural changes are minor, the substantial changes in potency clearly demonstrate the high level of sensitivity of the P2 position to steric modification. Within this initial set of dipeptide nitrile TgCPL inhibitors, leucine thus proved to be the most optimal residue in the P2 position for both potency and reduced selectivity for HsCPL.

Table 5. Inhibitory activity of trifluoroethylamine and cyclopropyl-nitrile analogs.

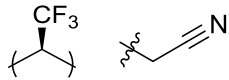
Name	X	R	TgCPL ^a IC ₅₀ (μM)	HsCPL ^b IC ₅₀ (μM)	Selectivity for HsCPL ^c
7n			0.25	0.28	0.9
19			0.66	0.59	1.1
18a			0.11	0.093	1.2
26			0.40	0.14	2.9
18b			0.16	0.084	1.9

See Table 2 for heading definitions.

Most CNS drugs do not tolerate more than 1 or 2 hydrogen bond donors. As shown in the LIGPLOT diagram from the co-crystal structure of HsCPL and compound **2** (Figure 2), the carbonyl of the P2-P3 amide is not actively engaged by the enzyme and therefore may be unnecessary. Replacement of this amide with the well-established trifluoroethylamine bioisostere offered an effective way to reduce our overall tPSA, greatly enhancing our chances for CNS penetration.^{43, 51-53} We found that the (R,S) diastereomer **19** gave a substantial drop in overall potency for both cathepsins (Table 5). The (S,S) diastereomer **18a**, however, doubled the potency against both the *Toxoplasma* and human enzymes, providing the most potent nitrile-based inhibitor to date against TgCPL with an IC₅₀ = 110 nM. This diastereomeric preference is consistent with literature reports of other dipeptide cathepsin inhibitors incorporating the trifluoroethyl amine bioisostere.⁴³

Table 6. Metabolic stability of select analogs in mouse liver microsomes.

Compound	R ₁	X	R ₂	MLM t _{1/2} (min)
7h	3-CF ₃			37
7n	4-F			>60

18a	4-F		4.4
18b	4-F		22

The metabolic stability of our dipeptide nitrile series was initially evaluated in mouse liver microsomes (MLM) to assess suitability for future in vivo studies and to further guide our design. Compound **7h** was evaluated to benchmark the dipeptide nitrile series (**Table 6**). We observed that compound **7h** had a reasonably long half-life (37 min). This parameter was further improved to >60 min with less lipophilic compound **7n**, despite several metabolic liabilities predicted by SMARTCyp (**Figure 5**).⁵⁴ Interestingly, while replacement of the P2 amide with a trifluoroethylamine (**18a**) removed an amide that could be a metabolic liability, the half-life in mouse liver microsome decreased to 4.4 minutes. It is likely that the increased lipophilicity simply enhanced binding to metabolizing enzymes. Two of the most likely positions for metabolism of **18a** are oxidation alpha to the nitrile warhead and hydrolysis of the P1 amide bond.⁵⁴ The incorporation of a cyclopropyl at the P1 position serves to block this site from oxidation and to slow hydrolysis of the P1 amide, a strategy successfully used in the development of odanacatib and other inhibitors of human cathepsins.^{51, 53, 55} Cyclopropyl analog **18b** indeed provided a significantly improved MLM half-life of 22 min, affording a compound more suitable for further in vivo analysis. It also retained potency for TgCPL, which is consistent with the predicted projection of the cyclopropyl group at P1 out into solvent (**Figure 4**).

Table 7. In Vivo Exposure of Compound **18b** Following IP Administration to Mice^a

Time Post-Dose	30 min	2 h	4 h	7 h
Plasma Conc. (ng/mL)	110	138	10	BLQ
Brain Conc. (ng/g)	54	BLQ	BLQ	BLQ

^a CD-1 mice were injected intraperitoneally with a single 10 mg/kg dose. The data shown are mean values from 2 mice at each time point. BLQ = Below Limit of Quantification.

Compound **18b** was advanced to an abbreviated in vivo pharmacokinetic study in mice (**Table 7**). Our main objective was to determine if this chemotype could penetrate the CNS. Significantly, we were able to detect compound in the brain, with a brain/plasma ratio of 0.5 at 30 minutes. Unfortunately, the overall levels in both brain and plasma were quite low, despite the fact that **18b** was shown to have good aqueous solubility (630 μ M) and excellent plasma stability (~100% parent remaining after 24h). The plasma levels and rapid disappearance indicates that this compound has a high volume of distribution, high clearance or both. Studies are currently underway to address this issue and to develop new analogs with improved pharmacokinetic profiles.

In summary, we have demonstrated for the first time that it is possible to modify a well established chemotype for inhibition of human cathepsins (dipeptide nitrile) and shift selectivity away from the human isoform and towards the *Toxoplasma gondii* isoform, a novel target for toxoplasmosis. Furthermore, we have demonstrated that the physical properties of the dipeptide can be adjusted to be more favorable for CNS penetration without loss of activity, particularly through reduction in tPSA and number of HBA. Key analogs in this campaign are summarized in **Figure 6**. Initially, our lead compound **2** was approximately 46-fold selective for HsCPL over TgCPL. We developed several compounds that either displayed equipotency for HsCPL and

TgCPL (**7n**), or exhibited slight selectivity (up to 3-fold) for TgCPL over HsCPL (**7h,7q**). Notably, compound **13** (Table 4) demonstrates the potential for achieving outright selectivity for TgCPL through the incorporation of a basic residue in the P2 position, an avenue we are exploring in future studies. Furthermore, we improved the potency of our inhibitors for the *T. gondii* enzyme from 2 μM to as low as 115 nM. Although we successfully demonstrated that compound **18b** can penetrate the blood brain barrier, it also exhibits rapid clearance in vivo. Current endeavors in our lab are aimed at further defining the pharmacophore for TgCPL via optimization of the P3 and P2 positions. Additionally, we are improving the pharmacokinetic profile for these inhibitors, so they may be advanced to in vivo murine infection studies in order to establish proof-of-concept that TgCPL is a viable target for treating the chronic form of toxoplasmosis.

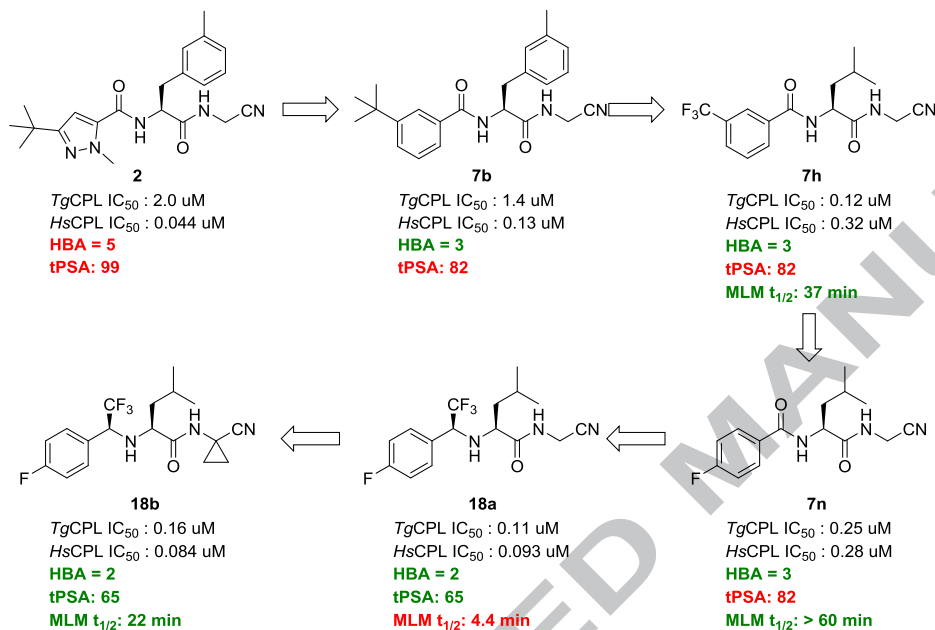


Figure 6. Key compounds in the optimization of **2** for TgCPL potency, metabolic stability, and a CNS-penetrant profile.

Acknowledgements

This work was supported by NIAID of the National Institutes of Health under award number R21/R33AI127492 (V.B.C. and S.D.L.). Its contents are solely the responsibility of the authors and do not necessarily represent the official views of the NIH. V.B.C. and S.D.L. were also supported by a grant from the Center for Discovery of New Medicines, University of Michigan. J.D.Z. acknowledges support from the University of Michigan Pharmacological Sciences Training Program (PSTP) training grant (T32-GM007767), and the Rackham Merit Fellowship (RMF). N.A.D. received support from the National Science Foundation (NSF DBI– #1263079), and National Institutes of Health (NIH/NIGMS GM007717).

References:

1. Furtado JM, Smith JR, Belfort R, Jr., Gattley D, Winthrop KL. Toxoplasmosis: a global threat. *J Glob Infect Dis.* 2011;3(3): 281-284.
2. Montoya JG, Remington JS. Management of *Toxoplasma gondii* infection during pregnancy. *Clin Infect Dis.* 2008;47(4): 554-566.

3. Scallan E, Hoekstra RM, Angulo FJ, et al. Foodborne illness acquired in the United States--major pathogens. *Emerg Infect Dis*. 2011;17(1): 7-15.
4. Jones JL, Parise ME, Fiore AE. Neglected parasitic infections in the United States: toxoplasmosis. *Am J Trop Med Hyg*. 2014;90(5): 794-799.
5. Parise ME, Hotez PJ, Slutsker L. Neglected parasitic infections in the United States: needs and opportunities. *Am J Trop Med Hyg*. 2014;90(5): 783-785.
6. Mendez OA, Koshy AA. *Toxoplasma gondii*: Entry, association, and physiological influence on the central nervous system. *PLoS Pathog*. 2017;13(7): e1006351.
7. Wohlfert EA, Blader IJ, Wilson EH. Brains and Brawn: *Toxoplasma* Infections of the Central Nervous System and Skeletal Muscle. *Trends in Parasitology*. 2017;33(7): 519-531.
8. Flegr J. Schizophrenia and *Toxoplasma gondii*: an undervalued association? *Expert Rev Anti Infect Ther*. 2015;13(7): 817-820.
9. Sutherland AL, Fond G, Kuin A, et al. Beyond the association. *Toxoplasma gondii* in schizophrenia, bipolar disorder, and addiction: systematic review and meta-analysis. *Acta Psychiatr Scand*. 2015;132(3): 161-179.
10. Flegr J. How and why *Toxoplasma* makes us crazy. *Trends in Parasitology*. 2013;29(4): 156-163.
11. Smith JE. A ubiquitous intracellular parasite: the cellular biology of *Toxoplasma gondii*. *Int J Parasitol*. 1995;25(11): 1301-1309.
12. Chorlton SD. *Toxoplasma gondii* and schizophrenia: a review of published RCTs. *Parasitol Res*. 2017;116(7): 1793-1799.
13. Saadatnia G, Golkar M. A review on human toxoplasmosis. *Scand J Infect Dis*. 2012;44(11): 805-814.
14. Liu Q, Wang ZD, Huang SY, Zhu XQ. Diagnosis of toxoplasmosis and typing of *Toxoplasma gondii*. *Parasit Vectors*. 2015;8: 292.
15. Sajid M, McKerrow JH. Cysteine proteases of parasitic organisms. *Mol Biochem Parasitol*. 2002;120(1): 1-21.
16. Ang KK, Ratnam J, Gut J, et al. Mining a cathepsin inhibitor library for new antiparasitic drug leads. *PLoS Negl Trop Dis*. 2011;5(5): e1023.
17. Beaulieu C, Isabel E, Fortier A, et al. Identification of potent and reversible cruzipain inhibitors for the treatment of Chagas disease. *Bioorganic & Medicinal Chemistry Letters*. 2010;20(24): 7444-7449.
18. Larson ET, Parussini F, Huynh MH, et al. *Toxoplasma gondii* cathepsin L is the primary target of the invasion-inhibitory compound morpholinurea-leucyl-homophenyl-vinyl sulfone phenyl. *J Biol Chem*. 2009;284(39): 26839-26850.
19. Di Cristina M, Dou Z, Lunghi M, et al. *Toxoplasma* depends on lysosomal consumption of autophagosomes for persistent infection. *Nat Microbiol*. 2017;2: 17096.
20. Barclay J, Clark AK, Ganju P, et al. Role of the cysteine protease cathepsin S in neuropathic hyperalgesia. *Pain*. 2007;130(3): 225-234.
21. Schirmeister T, Kaeppler U. Non-peptidic inhibitors of cysteine proteases. *Mini Rev Med Chem*. 2003;3(4): 361-373.
22. Turk V, Stoka V, Vasiljeva O, et al. Cysteine cathepsins: from structure, function and regulation to new frontiers. *Biochim Biophys Acta*. 2012;1824(1): 68-88.
23. Grzonka Z, Jankowska E, Kasprzykowski F, et al. Structural studies of cysteine proteases and their inhibitors. *Acta Biochim Pol*. 2001;48(1): 1-20.
24. Stoka V, Turk B, Turk V. Lysosomal cysteine proteases: Structural features and their role in apoptosis. *Iubmb Life*. 2005;57(4-5): 347-353.
25. Lankelma JM, Voorend DM, Barwari T, et al. Cathepsin L, target in cancer treatment? *Life Sci*. 2010;86(7-8): 225-233.
26. McGrath ME. The lysosomal cysteine proteases. *Annu Rev Biophys Biomol Struct*. 1999;28: 181-204.
27. Tsuge H, Nishimura T, Tada Y, et al. Inhibition mechanism of cathepsin L-specific inhibitors based on the crystal structure of papain-CLIK148 complex. *Biochem Biophys Res Commun*. 1999;266(2): 411-416.

28. Siklos M, BenAissa M, Thatcher GRJ. Cysteine proteases as therapeutic targets: does selectivity matter? A systematic review of calpain and cathepsin inhibitors. *Acta Pharm Sin B*. 2015;5(6): 506-519.
29. Andrews KT, Fisher G, Skinner-Adams TS. Drug repurposing and human parasitic protozoan diseases. *Int J Parasitol Drugs Drug Resist*. 2014;4(2): 95-111.
30. Inc. CCG. Molecular Operating Environment (MOE), 2013.08 2015.
31. Asaad N, Bethel PA, Coulson MD, et al. Dipeptidyl nitrile inhibitors of Cathepsin L. *Bioorganic & Medicinal Chemistry Letters*. 2009;19(15): 4280-4283.
32. Frizler M, Stirnberg M, Sisay MT, Gutschow M. Development of nitrile-based peptidic inhibitors of cysteine cathepsins. *Curr Top Med Chem*. 2010;10(3): 294-322.
33. Schmitz J, Furtmann N, Ponert M, et al. Active Site Mapping of Human Cathepsin F with Dipeptide Nitrile Inhibitors. *ChemMedChem*. 2015;10(8): 1365-1377.
34. Frizler M, Lohr F, Furtmann N, Klas J, Gutschow M. Structural optimization of azadipeptide nitriles strongly increases association rates and allows the development of selective cathepsin inhibitors. *J Med Chem*. 2011;54(1): 396-400.
35. Powers JC, Asgian JL, Ekici OD, James KE. Irreversible inhibitors of serine, cysteine, and threonine proteases. *Chem Rev*. 2002;102(12): 4639-4750.
36. Vicik R, Busemann M, Baumann K, Schirmeister T. Inhibitors of cysteine proteases. *Curr Top Med Chem*. 2006;6(4): 331-353.
37. Siklos M, BenAissa M, Thatcher GR. Cysteine proteases as therapeutic targets: does selectivity matter? A systematic review of calpain and cathepsin inhibitors. *Acta Pharm Sin B*. 2015;5(6): 506-519.
38. Borisek J, Vizovisek M, Sosnowski P, et al. Development of N-(Functionalized benzoyl)-homocycloleucyl-glycinonitriles as Potent Cathepsin K Inhibitors. *Journal of Medicinal Chemistry*. 2015;58(17): 6928-6937.
39. Hardegger LA, Kuhn B, Spinnler B, et al. Systematic investigation of halogen bonding in protein-ligand interactions. *Angew Chem Int Ed Engl*. 2011;50(1): 314-318.
40. McGrath ME, Klaus JL, Barnes MG, Bromme D. Crystal structure of human cathepsin K complexed with a potent inhibitor. *Nat Struct Biol*. 1997;4(2): 105-109.
41. Greenspan PD, Clark KL, Tommasi RA, et al. Identification of dipeptidyl nitriles as potent and selective inhibitors of cathepsin B through structure-based drug design. *Journal of Medicinal Chemistry*. 2001;44(26): 4524-4534.
42. Bromme D, Bonneau P, Lachance P, Storer AC. Engineering the S2 Subsite Specificity of Human Cathepsin-S to a Cathepsin-L-Like and Cathepsin-B-Like Specificity. *J Cell Biochem*. 1994: 152-152.
43. Black WC, Bayly CI, Davis DE, et al. Trifluoroethylamines as amide isosteres in inhibitors of cathepsin K. *Bioorganic & Medicinal Chemistry Letters*. 2005;15(21): 4741-4744.
44. Gauthier JY, Chauret N, Cromlish W, et al. The discovery of odanacatib (MK-0822), a selective inhibitor of cathepsin K. *Bioorganic & Medicinal Chemistry Letters*. 2008;18(3): 923-928.
45. O'Shea PD, Chen CY, Gauvreau D, et al. A Practical Enantioselective Synthesis of Odanacatib, a Potent Cathepsin K Inhibitor, via Triflate Displacement of an alpha-Trifluoromethylbenzyl Triflate. *J Org Chem*. 2009;74(4): 1605-1610.
46. Truong VL, Gauthier JY, Boyd M, Roy B, Scheiget J. Practical and efficient route to (S)-gamma-fluoroleucine. *Synlett*. 2005(8): 1279-1280.
47. Humphrey G, Chung CK, Rivera NR, Belyk KM. Asymmetric synthesis for preparing fluoroleucine alkyl esters. Google Patents; 2013.
48. Fanelli R, Martinez J, Cavelier F. Expedient Synthesis of Fmoc-(S)-Fluoroleucine and Late-Stage Fluorination of Peptides. *Synlett*. 2016;27(9): 1403-1407.
49. Smith HJ, Simons C. *Proteinase and peptidase inhibition : recent potential targets for drug development*. London ; New York: Taylor & Francis; 2002.
50. Bryant CM, Bunin BA, Kraynack EA, Patterson JW. N-cyanomethyl amides as protease inhibitors. 2001.

51. Gauthier JY, Chauret N, Cromlish W, et al. The discovery of odanacatib (MK-0822), a selective inhibitor of cathepsin K. *Bioorganic & Medicinal Chemistry Letters*. 2008;18(3): 923-928.
52. Sani M, Sinisi R, Molteni M, et al. The trifluoroethylamine function as peptide bond replacement. *Chim Oggi*. 2006;24(3): 42-43.
53. Gauthier JY, Black WC, Courchesne I, et al. The identification of potent, selective, and bioavailable cathepsin S inhibitors. *Bioorganic & Medicinal Chemistry Letters*. 2007;17(17): 4929-4933.
54. Rydberg P, Gloriam DE, Zaretski J, Breneman C, Olsen L. SMARTCyp: A 2D Method for Prediction of Cytochrome P450-Mediated Drug Metabolism. *ACS Med Chem Lett*. 2010;1(3): 96-100.
55. Braun MG, Castanedo G, Qin L, Salvo P, Zard SZ. Introduction of Trifluoroethylamine as Amide Isostere by C-H Functionalization of Heteroarenes. *Org Lett*. 2017;19(15): 4090-4093.

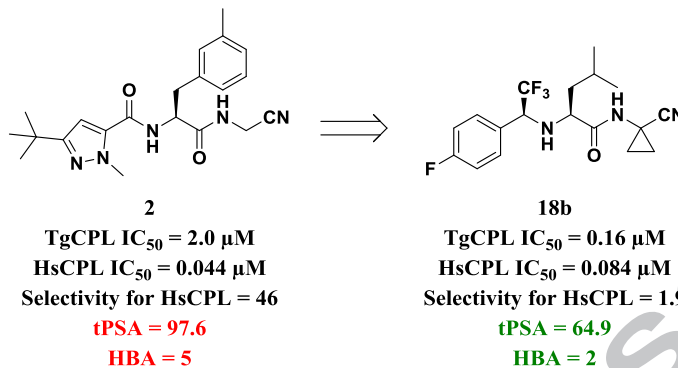
ACCEPTED MANUSCRIPT

Graphical Abstract:

Optimization of Dipeptidic Inhibitors of Cathepsin L for Improved *Toxoplasma gondii* Selectivity and CNS Permeability

Jeffery D. Zwicker, Nicolas A. Diaz, Alfredo J. Guerra, Paul D. Kirchhoff, Bo Wen, Duxin Sun, Vern B. Carruthers, and Scott D. Larsen

Leave this area blank for abstract info.



ACCEPTED MANUSCRIPT